Electronic Supplementary Information

Local Structures and Robust Oxygen Reduction Performances of TiN-Supported Bimetallic Pt-Cu Electrocatalysts for Fuel Cell

Hirosuke Matsui,[*a] Asako Shoji,[a] Chaoqi Chen,[a] Xiao Zhao,[b] Tomoya Uruga,[b,c] and Mizuki Tada[*a]

[a] Department of Chemistry, Graduate School of Science & Research Center for Materials Science & Integrated Research Consortium on Chemical Science & Institute for Advanced Study, Nagoya University, Furo, Chikusa, Nagoya, Aichi 464-8602 (Japan).
E-mail: matsui.hirosuke.x1@f.mail.nagoya-u.ac.jp
tada.mizuki.u6@f.mail.nagoya-u.ac.jp
[b] Innovation Research Center for Fuel Cells, The University of Electro-Communications, Chofu, Tokyo 182-8585 (Japan).
[c] Japan Synchrotron Radiation Research Center, SPring-8, Koto, Sayo, Hyogo 679-5198 (Japan)

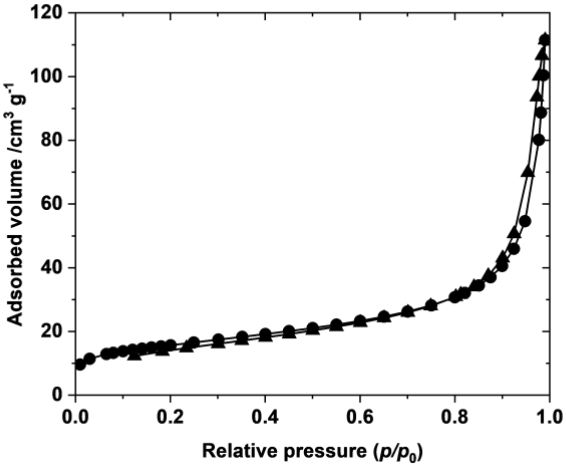

Fig. S1 N_2 adsorption isotherm at 77 K for the used TiN particles (NI-TIN-2, purity > 99.2%, EMJapan Co.). The symbols of ● and ▲ indicate the adsorption and desorption profiles of N_2, respectively.

Table S1 Examples of Pt and Cu loadings on the prepared PtCu-***X***/TiN catalysts (***X***: loaded Cu/Pt molar ratio)

Used Pt /wt%	**Loaded Pt /wt%**	**Used Cu /wt%**	**Loaded Cu /wt%**	***X***
20.0	17.7	0.0	0.0	0.0
20.1	17.9	0.0	0.0	0.0
19.5	15.3	1.6	1.0	0.2
19.5	14.2	1.6	1.1	0.2
19.3	14.3	2.5	1.8	0.3
19.3	15.7	2.5	2.3	0.4
18.5	14.5	6.9	5.1	1.0
18.6	13.1	7.0	4.8	1.0
18.6	14.6	7.0	5.7	1.1
18.5	14.2	6.9	5.7	1.1
18.3	14.2	8.3	6.4	1.3
18.3	14.0	8.5	6.6	1.3
18.5	14.5	8.5	7.0	1.4
17.6	13.8	8.5	6.9	1.4
17.5	12.4	12.1	9.8	2.4
17.6	12.4	12.3	9.6	2.3

The loading amounts of Pt and Cu onto the TiN support were estimated by the XRF-standard curve technique. The error of the calibration curve was within 1 %.

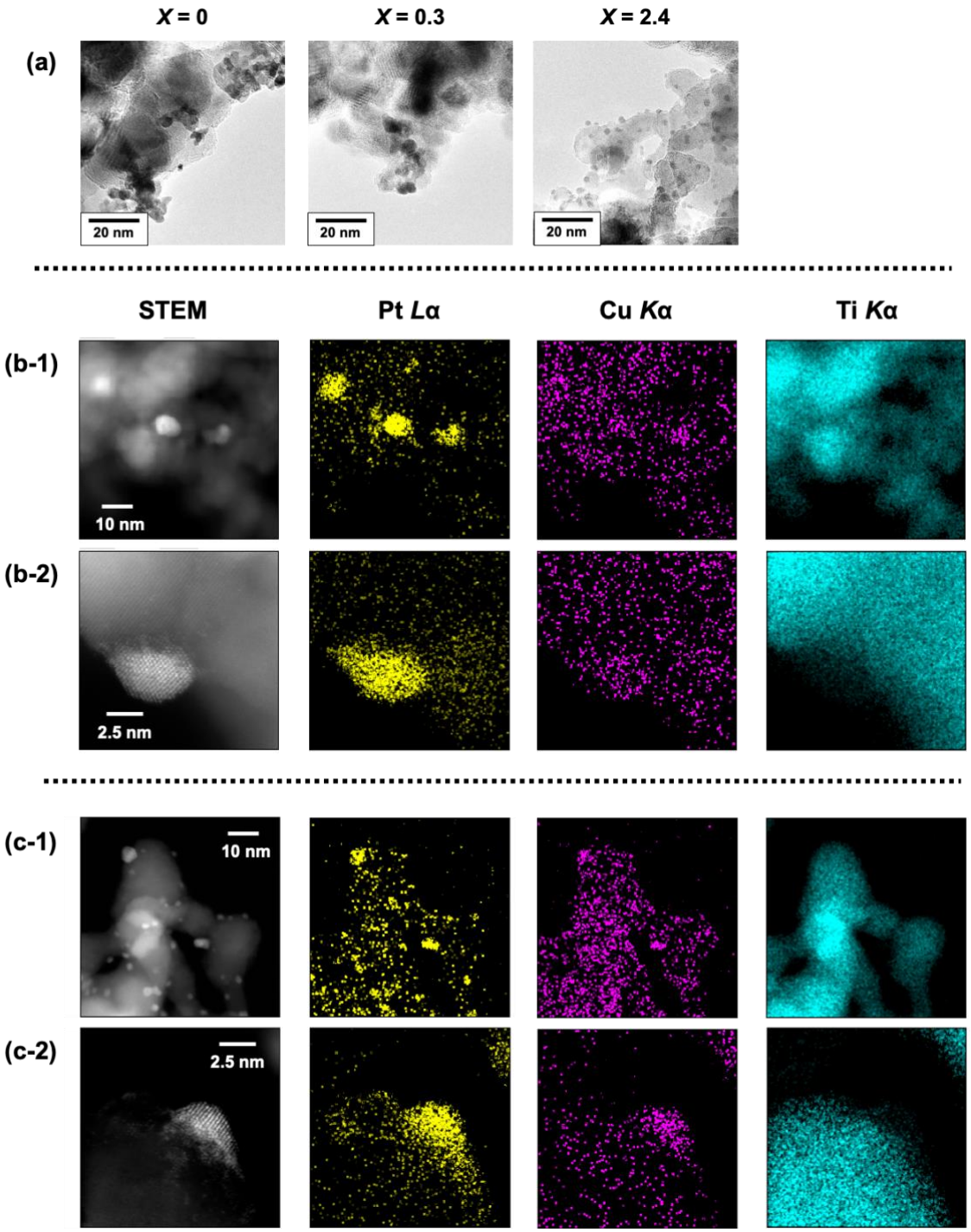

Fig. S2 (a) TEM images of the PtCu-***X***/TiN catalysts with different Cu/Pt loadings of ***X*** = 0, 0.3, and 2.4. (b, c) STEM-EDS mappings of Pt *L*α, Cu *K*α, and Ti *K*α for the prepared PtCu-***X***/TiN catalysts in (1) low and (2) high magnifications. (b) ***X*** = 0.2 (low Cu loading) and (c) ***X*** = 2.4 (high Cu loading).

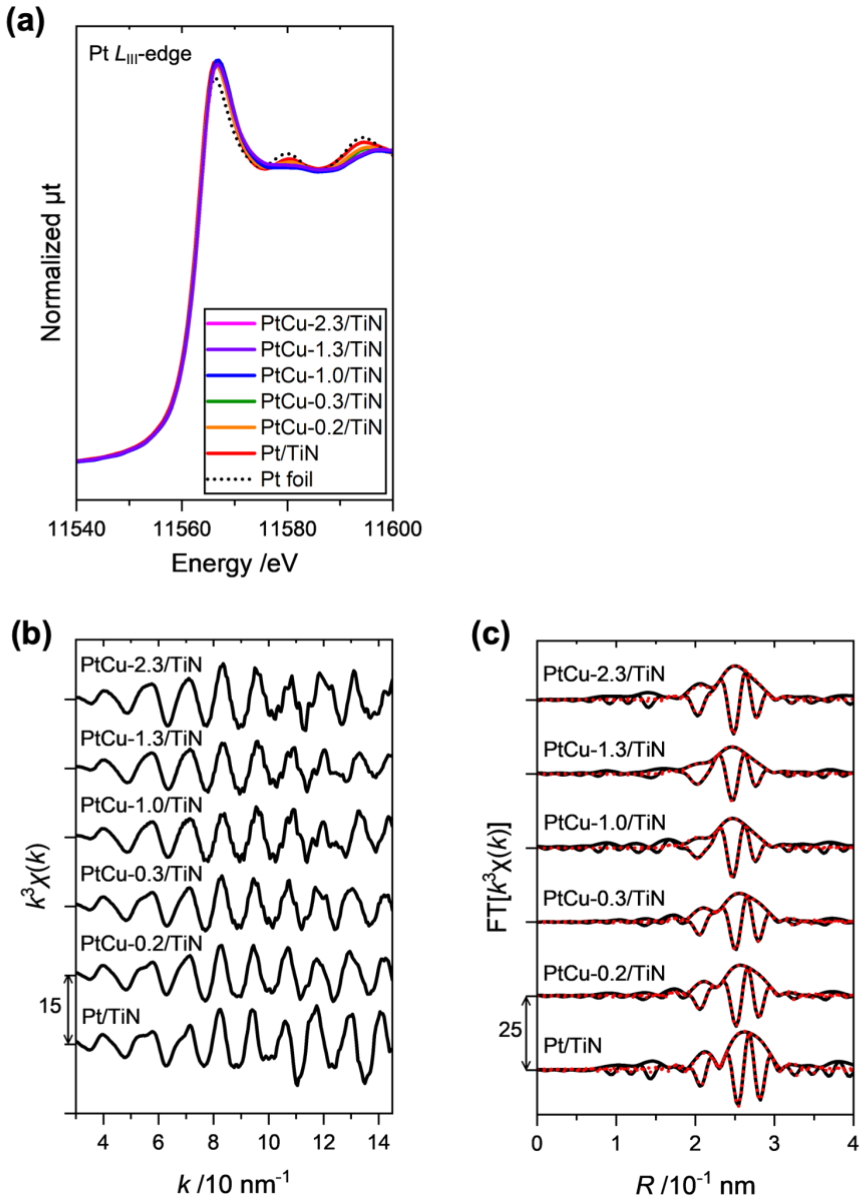

Fig. S3 (a) Normalized Pt L_{III}-edge XANES spectra, (b) k^3-weighted Pt L_{III}-edge EXAFS oscillations, and (c) k^3-weighted Pt L_{III}-edge EXAFS-Fourier transforms (FTs) for the PtCu-***X***/TiN catalysts (***X*** = 0−2.3). k = 3.0−14.5 × 10 nm^{-1}. Observed data: black lines, fitted data (fitting range: R = 1.9−3.1 × 10^{-1} nm): red lines.

Table S2. Curve-fitting results of Pt L_{III}-edge k^3-weight EXAFS-FTs for the PtCu-***X***/TiN catalysts (***X*** = 0−2.3)

Cu/Pt (XRF)	Shell	CN	R /10^{-1} nm	σ^2 /10^{-5} nm^2	ΔE_0 /eV	R-factor %
0	Pt-Pt	8.3±0.4	2.76±0.01	6.0±0.2	5.5±0.6	0.2
0.2	Pt-Pt	7.4±0.5	2.74±0.01	7.0±0.2	4.9±0.7	0.1
	Pt-Cu	1.1±0.2	2.68±0.02	9.0	7.4±3.5	
0.3	Pt-Pt	7.0±0.6	2.73±0.01	7.1±0.3	4.9±0.9	0.1
	Pt-Cu	1.3±0.2	2.66±0.02	9.0	5.7±3.6	
1.0	Pt-Pt	5.8±1.3	2.69±0.01	7.7±0.8	3.1±2.0	0.2
	Pt-Cu	2.5±0.4	2.68±0.02	9.0	7.2±3.5	
1.3	Pt-Pt	6.3±1.3	2.69±0.01	8.6±0.8	3.2±2.0	0.1
	Pt-Cu	2.4±0.8	2.66±0.02	9.0 ± 2.2	6.5±3.5	
2.3	Pt-Pt	6.7±1.6	2.70±0.01	6.9±0.9	2.7±2.3	0.3
	Pt-Cu	2.2±0.6	2.65±0.03	9.0	4.9±6.2	

S_0^2 was fixed to 0.94. k = 3−14.5×10 nm^{-1}. R = 1.9–3.1×10^{-1} nm. σ^2 values without error range were fixed to σ^2 obtained by the fitting analysis of PtCu-1.3/TiN.

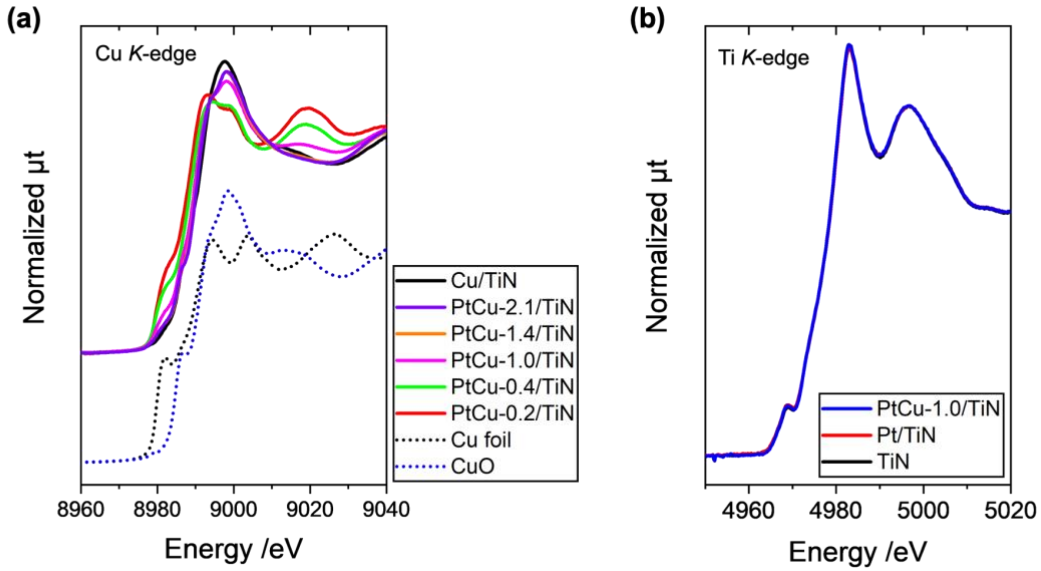

Fig. S4 (a) Normalized Cu *K*-edge XANES spectra of the PtCu-***X***/TiN catalysts (solid lines), Cu foil (black dotted line), and CuO (blue dotted line). (b) Normalized Ti *K*-edge XANES spectra of PtCu-1.0/TiN (blue), Pt/TiN (red), and TiN (black).

Table S3. The Gaussian curve-fitting results of Pt 4f and Cu $3p_{3/2}$ XPS peaks of PtCu-1.0/TiN in Fig. 4

Name	Peak	Binding energy /eV	Ratio to total area
Pt^{0+}	$4f_{7/2}$	71.3	0.41
	$4f_{5/2}$	74.6	0.31
Pt^{2+}	$4f_{7/2}$	74.0	0.13
	$4f_{5/2}$	77.3	0.10
Cu	Cu 3p	76.0	0.05

The energy gap and signal ratio of Pt $4f_{7/2}$ and $4f_{5/2}$ were defined as 3.3 eV and 4/3, respectively. Peak position and width were set as free parameters.

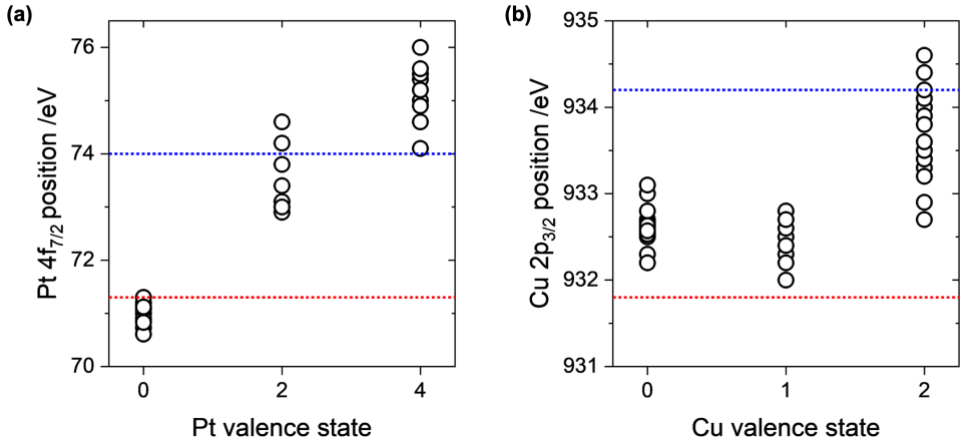

Fig. S5 The relationship of core-level shifts and reported valence states in (a) Pt $4f_{7/2}$ and (b) Cu $2p_{3/2}$. The values of plots were referred from the NIST XPS database.[33] (a) includes Pt (0), PtO (II), $Pt(OH)_2$ (II), and PtO_2 (IV). (b) includes Cu (0), Cu_2O (I), and CuO (II). Blue and red dotted lines indicate analyzed peak positions by the XPS analysis of the PtCu-1.0/TiN catalyst.

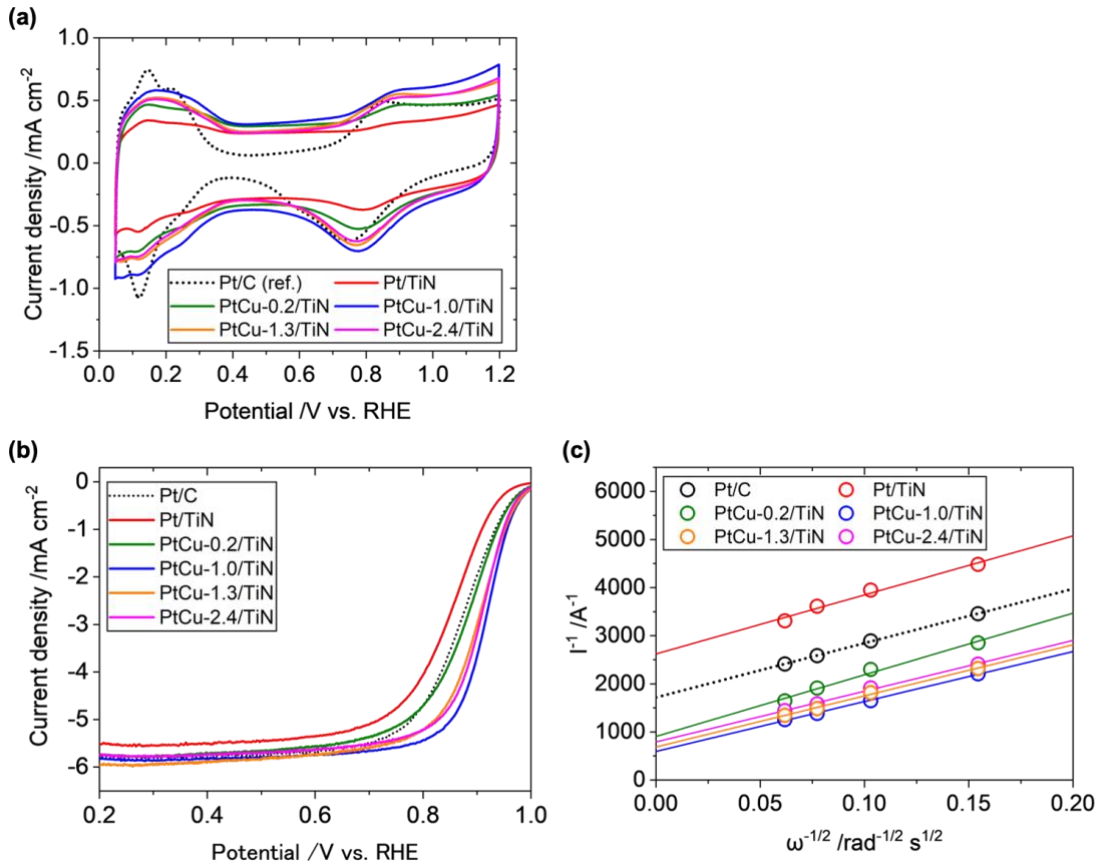

Fig. S6 (a) CV profiles of the prepared PtCu-***X***/TiN catalysts and a commercial Pt/C catalyst (TEC10E50E, TKK) as a reference (black dotted line). (b) Linear sweep voltammograms (the rotary rate of working electrode (WE) at 1600 rpm) and (c) Koutecký-Levich plots at the WE rotary rates of 400, 900, 1600, and 2500 rpm for the PtCu-***X***/TiN catalysts (***X*** = 0 (red), 0.2 (green), 1.0 (blue), 1.3 (orange), and 2.4 (pink)).

Table S4. Estimated ECSA, SSA, and MSA for the prepared PtCu-***X***/TiN catalysts (***X*** = 0−2.4) and a commercial Pt/C catalyst (TEC10E50E, TKK),

Loaded Cu/Pt*	**ECSA /m^2 g^{-1}**	**SSA /mA cm_{Pt}^{-2}**	**MSA /A mg_{Pt}^{-1}**
0.0	20.4 ± 0.5	0.86 ± 0.14	0.17 ± 0.02
0.2 ± 0.1	33.4 ± 3.3	1.28 ± 0.14	0.44 ± 0.08
1.0 ± 0.1	54.6 ± 2.7	1.58 ± 0.05	0.86 ± 0.06
1.3 ± 0.1	54.4 ± 4.3	1.24 ± 0.17	0.68 ± 0.13
2.4 ± 0.1	56.4 ± 5.4	1.31 ± 0.11	0.73 ± 0.12
Pt/C (TEC10E50E, TKK)	68.2	0.25	0.17

*Several samples were evaluated and differences in the loaded Cu/Pt in the samples were presented by error range (± 0.1).

Table S5. Comparison of the ORR performance for the Pt/TiN-based electrocatalysts in electrochemical RDE studies from literature and this work,

Catalyst	ECSA /m^2 g^{-1}	MSA /A mg^{-1}	SSA /mA cm^{-2}	ref.
TiNiN@Pt	97	0.83	0.49	24
$Ti_{0.9}Cu_{0.1}N$@Pt/NCNT	100.2	1.06	0.69	25
Pt_3Cu nanoframe/TiN architecture	45.7	5.32	2.43	26
Pt/$Ti_{0.9}Co_{0.1}N$	54.9	0.46	0.54	27
PtCu-1.0/TiN	**54.6**	**0.86**	**1.58**	**This work**

Table S6. Comparison of the ORR performance for the Pt/TiN-based electrocatalysts in PEFC MEA from literature and this work,

Catalyst	**ECSA /m^2 g^{-1}**	**Mass-specific power density /W mg^{-1}**	**ref.**
Pt/TiN	56	—	38
Pt/hierarchical TiN nanostructured thin film	42.3	0.3	39
PtCu-1.0/TiN	**60.3**	**1.5**	**This work**

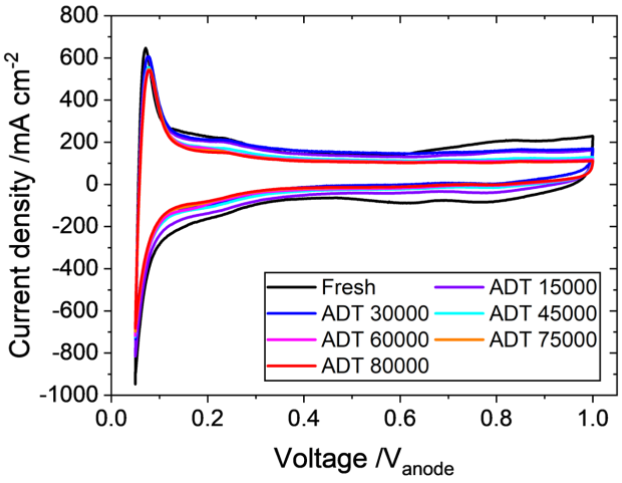

Fig. S7 The CV profiles of a prepared three-layered MEA using PtCu-1.0/TiN as the cathode (0.11 mg_{Pt} cm^{-2}, 3 cm × 3 cm) and changes in the CV profiles during ADT cycles (0−80000 cycles; 0.6 V and 1.0 V for 3 s each under N_2 at the cathode).